

# Dynamic Self-Assembly of Polymer Colloids To Form Linear Patterns

Matthew A. Ray,<sup>†</sup> Hyungsoo Kim,<sup>‡</sup> and Li Jia<sup>\*,†,‡</sup>

Department of Chemistry and Emulsion Polymers Institute, Lehigh University,  
Bethlehem, Pennsylvania 18015

Received January 20, 2005. In Final Form: April 2, 2005

Ⓜ This paper contains enhanced objects available on the Internet at <http://pubs.acs.org/journals/langd5>.

A dynamic self-assembling process is reported which involves drying a droplet of *positively charged* colloidal suspension on a flat *negatively charged* hydrophilic surface. This extremely simple method affords lines of colloidal particles with regular 1.5–4.5  $\mu\text{m}$  line spacing and smaller than 2  $\mu\text{m}$  line width over a broad surface area. The ordered region diffracts light to display an iridescent appearance and generates first-order diffraction spots when illuminated by a He–Ne laser. A periodic stick–slip motion of the drying liquid front is observed during the drying process using optical microscopy. The periodic motion must be related to the periodic particle deposition. We propose that the simultaneous deposition of the particles at a fixed distance (i.e., the line spacing) behind the previous line of particles where the contact line is pinned is in turn responsible for the periodic stick–slip motion. The key distinguishing feature of the present system is the attractive interaction between the particles and the surface, which instigates the periodicity of the particle deposition.

## Introduction

Dewetting is a process that has drawn lasting scientific interest.<sup>1</sup> The events of surface pinning and convective flow during the dewetting process of a droplet of a colloidal suspension on a flat surface have received renewed interests because they can be potentially harnessed as an extremely simple way for surface patterning.<sup>2</sup> A variety of patterns generated by this process have been observed on mica and glass.<sup>3–6</sup> The patterns generally lack long-range order and exceed the length scale of 10  $\mu\text{m}$ . In all of the previous studies, the substrate surface and the colloidal particles both have a negative surface charge and, therefore, electrostatically repel each other. The theoretical studies on evaporating droplets on flat surfaces simply treat the deposition as a passive process by discounting the surface–particle interaction.<sup>7–10</sup> This caused our interest in studying systems where the substrate surface and the particles are oppositely charged. We report here that drying a droplet of *positively charged* colloidal suspension on a flat *negatively charged* hydrophilic surface results in lines of colloidal particles with regular line spacing over a broad surface area (Figure 1). The mechanism of the dynamic self-assembly process will be discussed.

## Experimental Methods

**Sample Preparation.** Poly(styrene-*co*-vinylimidazole) latex particles were prepared by surfactant free emulsion copolymerization.<sup>11</sup> The average particle diameters were measured using transmission and scanning electron microscopy (Phillips 420T, JEOL 6300f) and were found to be 258 nm with a narrow polydispersity index (PDI) of 1.003 and 391 nm with a PDI of 1.011. The particle suspension was diluted to appropriate sample concentrations with Milli-Q water. The pH of the dilute suspension was around 8. The imidazole groups on the surface of the particles ionize at this pH and bear a positive charge. The zeta potentials of the particles were measured (PenKem model 501 Lazer Zee Meter) and found to be  $+29.6 \pm 4.2$  mV (standard deviation, 18 measurements) for the 258 nm particles and  $+31.6 \pm 3.5$  mV (standard deviation, 25 measurements) for the 391 nm particles. The surfaces of silicon wafers or glass slides were cleaned with concentrated sulfuric acid followed by thorough rinsing. The linear pattern formed over a range of particle concentrations between 0.005 and 0.2 wt % solids. The pattern was formed by placing a single drop ( $\sim 38 \mu\text{L}$ ) of suspension onto a 12  $\times$  12 mm glass or silicon substrate. The substrate was immediately tilted in different directions to allow the drop to completely wet the surface. Once the surface was completely wetted, the substrate was typically placed at an angle of 10° with respect to the benchtop and allowed to dry in a covered Petri dish at room temperature. Typical drying times were 2–3 h.

For control experiments of the substrate surface charge, PDDA [poly(diallyldimethylammonium chloride), Aldrich] was used to switch the surface charge from negative to positive. To accomplish this, cleaned glass substrates were dipped into 5.0 wt % PDDA for 30 min, thoroughly rinsed with deionized water, and blown dry with a nitrogen jet. These substrates were then used in the procedure outlined above. For control experiments of the particle charge, 128 nm poly(styrene-*co*-styrenesulfonate) latex particles were prepared by surfactant free emulsion copolymerization. The particles had a PDI of 1.018 and a zeta potential of  $-71.2 \pm 9.7$  mV (standard deviation, six measurements). The particles were diluted to 0.03 wt % and used in the procedure outlined above. Polystyrene latex particles with an average diameter of 234 nm, a PDI of 1.000, and a zeta potential of  $-54.2 \pm 1.7$  mV (standard deviation, 12 measurements) were obtained (DOW LS-1047-E)

\* To whom the correspondence should be addressed. E-mail: [lij4@lehigh.edu](mailto:lij4@lehigh.edu).

<sup>†</sup> Department of Chemistry, Lehigh University.

<sup>‡</sup> Emulsion Polymers Institute, Lehigh University.

(1) de Gennes, P. G. *Rev. Mod. Phys.* **1985**, *57*, 827–863.

(2) Deegan, R. D.; Bkajin, O.; Dupont, T. F.; Huber, G.; Nagel, S. R.; Witten, T. A. *Nature* **1997**, *389*, 827–829.

(3) Deegan, R. D. *Phys. Rev. E* **2000**, *61*, 475–485.

(4) Nagayama, K. *Colloids Surf., A* **1996**, *109*, 363–374.

(5) Micheletto, R.; Fukuda, H.; Ohtsu, M. *Langmuir* **1995**, *11*, 3333–3336.

(6) Abkarian, M.; Nunes, J.; Stone, H. A. *J. Am. Chem. Soc.* **2004**, *126*, 5978–5979.

(7) Adachi, E.; Dimitrov, A. S.; Nagayama, K. *Langmuir* **1995**, *11*, 1057–1060.

(8) Dushkin, C. D.; Lazarov, G. S.; Kotsev, S. N.; Yoshimura, H.; Nagayama, K. *Colloid Polym. Sci.* **1999**, *277*, 914–930.

(9) Hu, H.; Larson, R. G. *J. Phys. Chem. B* **2002**, *106*, 1334–1344.

(10) Fischer, B. *J. Langmuir* **2002**, *18*, 60–67.

(11) Tauer, K.; Deckwer, R.; Kühn, I.; Schellenberg, C. *Colloid Polym. Sci.* **1999**, *277*, 607–626.

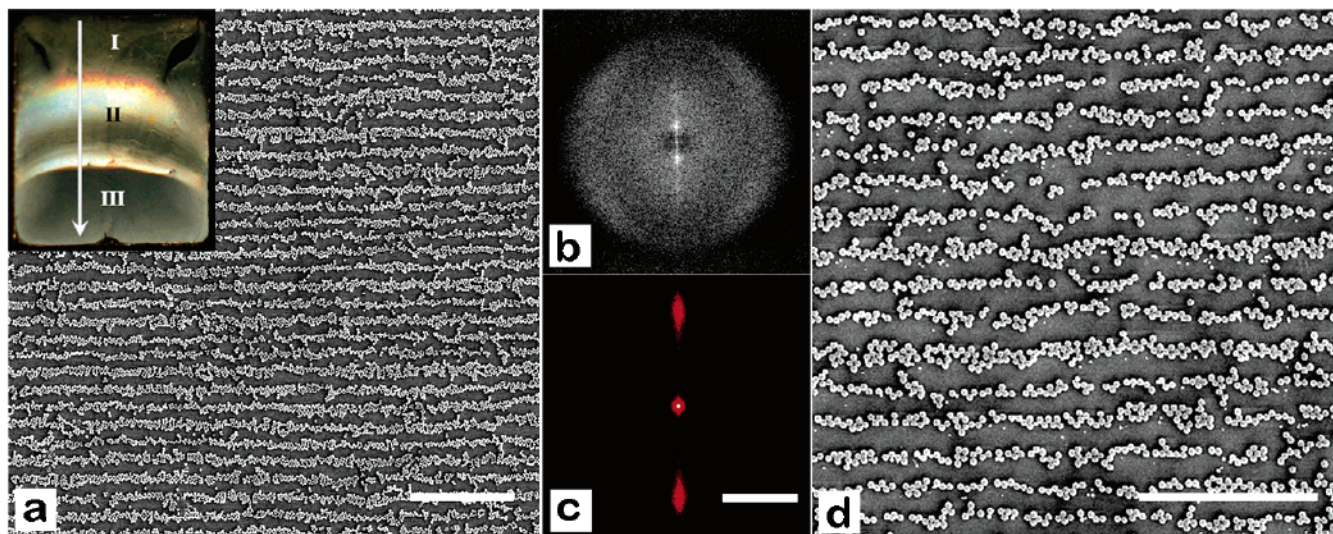


**Figure 1.** (a) SEM image of the linear pattern found in region II using 258 nm particles on glass. Scale bar: 10  $\mu\text{m}$ . The inset (12 mm wide) shows the three regions observed with a typical sample. The arrow indicates the liquid receding direction during the drying process. (b) FFT of the linear pattern in micrograph a. Notice the intense spots which were used to measure the center-to-center line spacing. The halo is caused by the particle diameter. (c) Laser diffraction pattern of a similar patterned region.  $\lambda$ , 632.8 nm; projection length, 25 cm; scale bar, 10 cm. (d) SEM image showing an area of region II using 391 nm particles on glass. Scale bar: 10  $\mu\text{m}$ .

Ⓜ A movie depicting the ordering process in MPEG format is available.

and diluted to 0.02 wt %. These particles were also used to pattern substrates as outlined above. The results of the control experiments may be seen in the Supporting Information.

**Microscopy and Analysis.** The particle patterns were analyzed with scanning electron microscopy (JEOL, 6300f). Video and color digital images of the ordering process were recorded by a charge-coupled device camera attached to the optical microscope (Olympus, BH2). For this procedure the entire microscope was tilted to  $\sim 10^\circ$ , and the same sample preparation procedure was used except that the substrate was placed on the microscope stage to dry. All of the scanning electron microscope (SEM) samples were sputter-coated with a thin layer of gold palladium alloy (Polaron E5100 SEM coating unit) to make the surface conductive. The repeat distance of the striped pattern was analyzed by two-dimensional fast Fourier transform (FFT). Fourier transform image analysis was performed using Scion Image for Windows release Beta 4.0.2. By measuring the distance between the center, defined as pixel (256, 256) in a  $512 \times 512$  pixel image, and the prominent points in the transformed image, the periodicity in the original image can be calculated. The distance in the transformed image can be related to the distance in the original image using the equation  $d = 512/r$ , where  $d$  is the center-to-center line spacing in the original image and  $r$  is the distance in pixels from the center of the transformed image to the center of the prominent points. Laser diffraction patterns were obtained by illuminating samples at normal incidence with a 5 mW helium–neon laser (Hughes) and projecting the resulting diffraction patterns onto a screen at a projection length of 25 cm. Images of the diffraction patterns were taken using a digital camera (Cannon, G3). Analysis of the diffraction pattern in Figure 1c yields a line spacing of 1.37  $\mu\text{m}$ .

## Results and Discussion

In the present study, poly(styrene-*co*-vinylimidazole)-latex particles with average diameters of 258 and 391 nm were used. The particles are substantially positively charged as indicated by zeta-potential measurement. The surfaces of silicon wafers or glass slides bear a negative charge density of roughly  $-0.32 \text{ mC/m}^2$ .<sup>12</sup> The self-assembling process was effected by simply placing a drop of the colloidal suspension on the substrate and allowing

the wetted surface to dry. After an induction period which results in a region of randomly absorbed colloidal particles (Figure 1, inset region I), the process resulted in deposition of lines of particles *parallel* to the air–substrate–liquid contact line with regular line spacing. Macroscopic directionality of the linear pattern running all the way across the width of the substrate can be achieved by placing the substrate at a small tilt angle with respect to the horizontal benchtop. If the substrate is left flat, the pattern is in the form of concentric circles.

The center-to-center line spacing of the pattern can be determined by two-dimensional FFT of the SEM images (Figure 1b).<sup>13</sup> As the pattern begins to emerge at the end of region I, the line spacing is wide and gradually decreases to become roughly constant throughout the rest of region II (Figure 2) until the onset of a third region (Figure 1, inset region III). Region III is characterized by randomly adsorbed particles or an area of close-packed particle monolayers and multilayers depending on the initial droplet concentration. The end of regular line formation is likely because the concentration of the particles in the droplet is changed out of the range for pattern formation by particle deposition or solvent evaporation. The optimal initial concentration ranges from 0.005 to 0.02 wt % particle solids. Within this range, the largest area of region II is observed on the substrate. The upper limit of initial concentration for line formation is approximately 0.2 wt % particle solids. Parenthetically, because the particle suspension concentrations used in these experiments are quite dilute, random adsorption of oppositely charged colloids on the charged surface<sup>14,15</sup> occurs very slowly compared to the ordering process and, therefore, does not significantly interfere (see Supporting Information). The line widths within region II are examined by counting and averaging the number of particles in individual lines (Figure 2b). At low initial concentrations (0.005 and 0.01

(13) Gonzalez, R. C.; Woods, R. E. *Digital Image Processing*; Prentice: Upper Saddle River, NJ, 2002.

(14) Johnson, C. A.; Lenhoff, A. M. *J. Colloid Interface Sci.* **1996**, *179*, 587.

(15) Evans, J. W. *Rev. Mod. Phys.* **1993**, *65*, 1281.

(12) Behrens, S. H.; Grier, D. G. *J. Chem. Phys.* **2001**, *115*, 6716–6721.

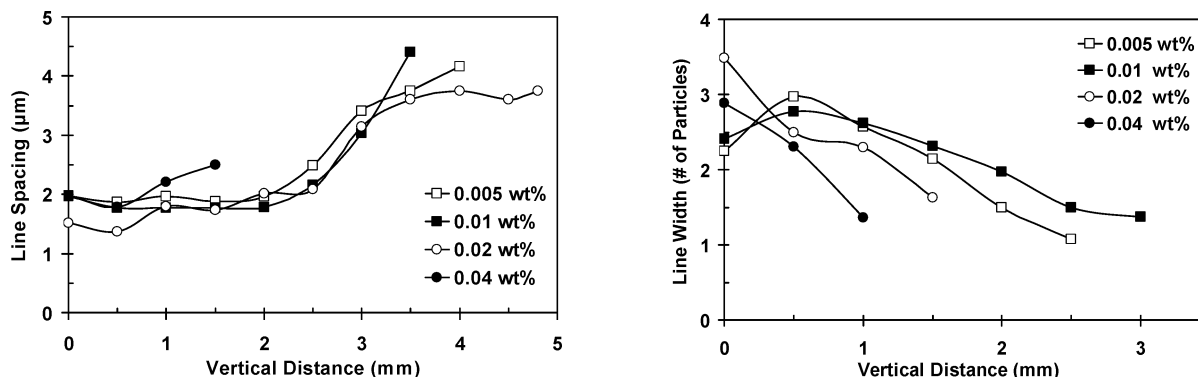


**Figure 2.** Change of line spacing (left) and change of individual line width (right) with the progression of the drying process for the 258 nm particle system on glass at different initial concentrations. The origin is placed in the center of the boundary between region II and region III and measurements are taken at 500  $\mu\text{m}$  intervals while moving toward region I, opposite of the arrow in the inset to Figure 1a.

wt %), the individual line width gradually increases, reaches a maximum, and then gradually decreases before the line pattern rather abruptly fades into region III with sparse randomly adsorbed particles. At the intermediate initial concentration near 0.02 wt %, the individual line width gradually increases, becomes an area of nearly continuous hexagonal close packed (HCP) monolayer, and then re-emerges before the appearance of region III with sparse randomly adsorbed particles. At high initial concentrations (0.04 wt %), the individual line width again gradually increases and then becomes a monolayer at the edge of region III with HCP monolayers and multilayers. These changes in the line width are possibly because the particle concentration within the droplet is not constant during the drying process due to two concurrent events, solvent evaporation and particle deposition.

The process of the pattern formation was monitored by optical microscopy with the substrate at a tilt angle of  $10^\circ$ . The contact line initially recedes quickly in part due to gravity shaping the drop on the tilted surface, resulting in region I. After advancing several millimeters, self-pinning<sup>3</sup> occurs and the region bearing the linear pattern starts to appear. There is no clear transition between region I and region II, instead the ordered lines emerge from the disorder in a smooth gradient. During the formation of a single line in region II, the contact line is temporarily pinned at a certain position. A point of the contact line will first recede to the next position. This immediately triggers the recession of the entire line to the next position (see the web-enhanced object at the end of the Figure 1 caption). The motion occurs with a regular period of  $5.32 \pm 2.07$  s (standard deviation, 126 measurements) during the ordering process for the 258 nm particles. The observed “stick–slip” behavior is remarkably similar to the classic dewetting study using a phonograph record blank as the substrate.<sup>16,17</sup> Compared to its initiation, the end of the line formation happens rather abruptly with the appearance of region III.

The optical microscopy study indicates that the deposition of the lines parallel to the contact line is due to the convective particle flow within the evaporating droplet and the “stick–slip” motion of the contact line. The remaining critical question is what causes the “stick–slip” motion to occur in such regular steps without pre-prepared linear surface features. To answer this question, we looked at a few variables that may affect the periodicity of the linear pattern. The initial colloidal suspension concentration appears to have no obvious effect on the

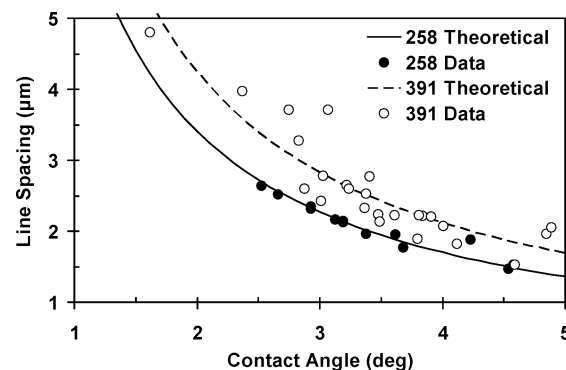


**Figure 3.** Effect of the contact angle on the line spacing of 258 and 391 nm particle patterns on glass fitted with the equation  $y = (D - h)/\tan(x)$ , where  $y$  is the line spacing,  $D$  is the particle diameter,  $h$  is the height of the pinning site, and  $x$  is the contact angle.

center-to-center line spacing. The line spacing is also independent of the substrate tilt angle between  $0$  and  $30^\circ$ . Variation of the evaporation rate by covering the drying substrate in a Petri dish or leaving it exposed to the ambient environment exerts no obvious effect of line spacing either, although a faster drying rate results in more defects bridging the adjacent lines. The only observed change of line spacing arises from the progress of the drying process (Figure 2). The line spacing is wide at the beginning of region II and gradually decreases to become roughly constant.

A careful examination of the change of the liquid height profile close to the contact line during the evaporative dewetting process provides important insights. First, the liquid height profile was accurately measured by optical interference microscopy<sup>18</sup> using a monochromatic light source. The contact angles at specific positions as the contact line moved down the substrate were calculated from the height profiles (see Supporting Information). FFT analysis of the optical micrographs was then performed to measure the line spacing just above the contact line region where a given contact angle was measured. The effect of the contact angle on the line spacing is shown in Figure 3.

The decrease of the line spacing with the increase of the contact angle allows us to propose the following mechanism for the formation of the linear periodicity. After the ordering process is initiated, the contact line is pinned on the back edge of the previously formed line at a height

(16) Oliver, J. F.; Huh, C.; Mason, S. G. *J. Adhes.* **1977**, *8*, 223–234.

(17) Huh, C.; Mason, S. G. *J. Colloid Interface Sci.* **1977**, *60*, 11–38.

(18) Hadjiishi, A.; Dimova, R.; Denkov, N. D.; Ivanov, I. B.; Borwanker, R. *Langmuir* **1996**, *12*, 6665–6675.

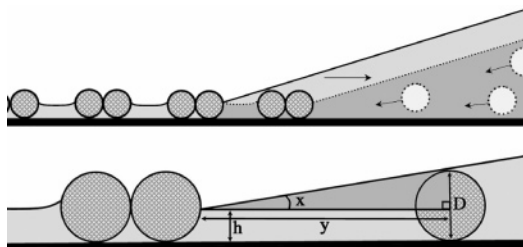


**Figure 4.** Top: Schematic illustration of the ordering process. Bottom: Geometry used to describe the ordering process.

lower than one particle diameter (Figure 4). Because the contact angle is very small, the liquid layer does not reach the height of one particle diameter until moving back one to a few  $\mu\text{m}$  from the contact line. Convective flow rushes particles into the wedge-shaped liquid layer, and at the location with the wedge thickness equal to or perhaps slight larger than the particle diameter, the particles are arrested by the surface and become immobile due to the attractive forces between the surface and the particles. Later in the process, when the contact angle increases, the particles are able to approach closer to the previous line where the drop edge is pinned, resulting in closer line spacing. By assuming that a given particle will become pinned when it encounters the liquid height equal to its diameter, the above model predicts the geometric relationship  $y = (D - h)/\tan(x)$ , where  $y$  is the line spacing in micrometers,  $x$  is the contact angle in degrees,  $D$  is the particle diameter in micrometers, and  $h$  is the pinning height in micrometers on the back of the previous line. The data of line spacing versus contact angle for both the 258 and 391 nm particles can be fitted with this equation (Figure 3). The curve fit produces an  $h$  value of  $0.139 \mu\text{m}$  for the 258 nm data and  $0.243 \mu\text{m}$  for the 391 nm data. These height values are consistent with what is expected if the contact line were being pinned on the backside of a ridge one diameter high.<sup>1</sup> We essentially assemble a grooved surface similar to the classic phonograph record example one line at a time.<sup>16,17</sup> The “groove” behind the contact line is assembled immediately before the contact line retracts and pins upon it. Once the first particle row forms, the order reproduces itself as the contact line propagates down the surface of the substrate.

The deposition of negatively charged particles on negatively charged glass surfaces to form HCP particle bands has been rather expensively studied by Nagayama et al. As control experiments, we reproduced their results. Further, when the surface charge of the substrate is

switched from negative to positive by adsorbing a layer of PDDA, both the 258 and 391 positive particles again form wide HCP particle bands with irregular band spacings similar to the negative particles on the negative surface. It is instructive to recall Nagayama’s study on the same-charged systems in comparison to the present oppositely charged system.<sup>4,7,8</sup> In their reports, bands with widths ranging from 10 to  $200 \mu\text{m}$  with irregular interband distances are formed. The particles are injected *past the contact line into the wetting film* by convective flow. The negative particles are *laterally mobile* in the wetting film until incorporated into the HCP lattice by capillary forces. No line or band is assembled behind the contact line before the contact line slips. Once it slips, the contact line cannot stop until a new self-pinning process is initiated and achieved. In our case, the particles stop and are *laterally immobile before they reach the contact line*. The differences between the same-charged systems and the oppositely charged systems indicate that without excluding the possible role of other attractive forces, the Coulombic attraction is critical for the linear pattern formation.

### Conclusions

We have shown that an ordered linear pattern can be conveniently produced requiring little surface preparation. The ordering process is a dynamic self-assembling process<sup>19</sup> involving deposition of particles by convective flow behind the contact line and the “stick–slip” motion of the contact line as observed by optical microscopy. We propose that the propagation wavelength of the “stick–slip” motion is stipulated by the wedge-shaped geometry of the liquid layer near the contact line and the size of the particles. The propagation mechanism relies on the immobilization of particles by attractive forces, particularly Coulombic attraction, as the particles are carried into close vicinity of the substrate surface by convective flow.

**Acknowledgment.** The authors thank the Center of Optical Technologies at Lehigh University for financial support. L.J. thanks the Du Pont Company for a Du Pont Young Professor Award.

**Supporting Information Available:** Results from the control experiments, description of contact angle measurement by optical interference, line width measurements, and rate of random sequential adsorption. This material is available free of charge via the Internet at <http://pubs.acs.org>.

LA050165R

(19) Whitesides, G. M.; Grzybowski, B. *Science* **2002**, *295*, 2418–2421.